NANO · MICRO
small

Supporting Information

for *Small*, DOI 10.1002/smll.202500288

Fluorination Induced Inversion of Helicity and Self-Assembly Into Cross-α Like Piezoelectric Amyloids by Minimalistic Designer Peptide

Sukantha Dey, Emily H. Field, Yuehui Wang, Kyunghoon Han, Rohit Kumar, Linda J. W. Shimon, Shuaijie Liu, Sarah Guerin, Joshua T. Berryman, Wei Ji, Nicholas P. Reynolds* and Santu Bera**

Supporting Information

Fluorination Induced Inversion of Helicity and Self-Assembly into Cross-α like Piezoelectric Amyloids by Minimalistic Designer Peptide

Sukantha Dey, Emily H. Field, Yuehui Wang, Kyunghoon Han, Rohit Kumar, Linda J. W. Shimon, Shuaijie Liu, Sarah Guerin, Joshua T. Berryman, Wei Ji, Nicholas P. Reynolds,* and Santu Bera**

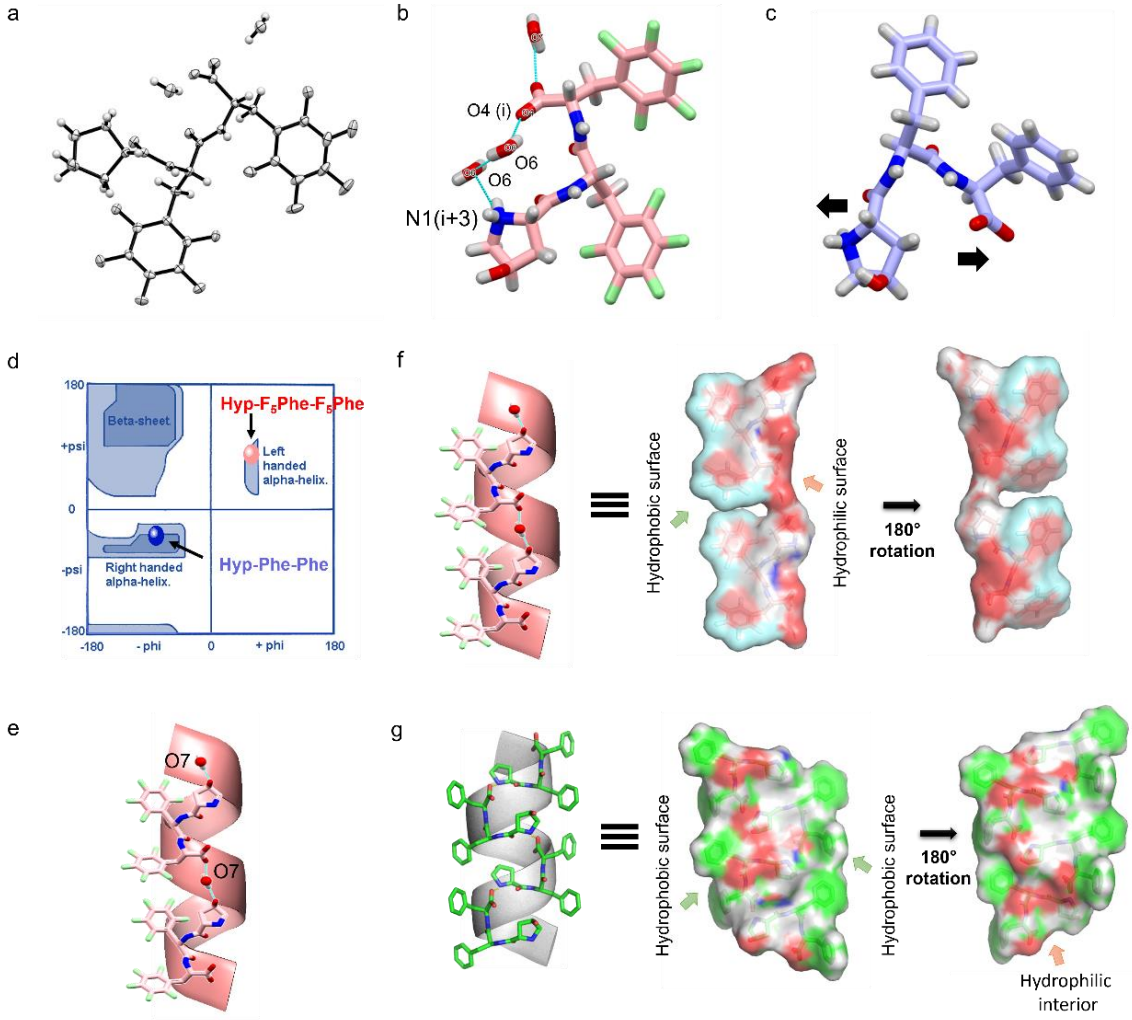

Figure S1. Crystal structure of Hyp-Phe-Phe vs Hyp-F_5Phe- F_5Phe. a) ORTEP diagram of the asymmetric unit of Hyp-F_5Phe-F_5Phe in 50% probability displacement ellipsoids. b) Asymmetric unit of Hyp-F_5Phe-F_5Phe with labelled the i and (i+3) residues along with connecting water oxygens. c) Asymmetric unit of Hyp-Phe-Phe. The black arrows indicating the two terminals i.e., i and (i+3) are

directed in opposite directions, thus no possibility for connection. d) Ramachandran plot of the allowed dihedral angles of Phe2 and F_5Phe2 residues of Hyp-Phe-Phe and Hyp-F_5Phe-F_5Phe in blue and pink, respectively, showing the preferences for right and left-handed helical conformation. e) Water (O7) connects individual peptide molecules in head-to-tail fashion through H-bonding and thus producing the extended columnar structure of helical strand. f,g) Surfaces of a single helix of Hyp-F_5Phe-F_5Phe (f) and Hyp-Phe-Phe (g) are shown by 180° rotations. For Hyp-F_5Phe-F_5Phe, one face of helix is hydrophobic through extending aromatic rings while the other face is hydrophilic involving backbone connected with water molecules. For Hyp-Phe-Phe, figures show two faces of the helix are hydrophobic in nature by exposing aromatic ring of Phe residues. The interion is hydrophilic in nature by extending the amide groups.

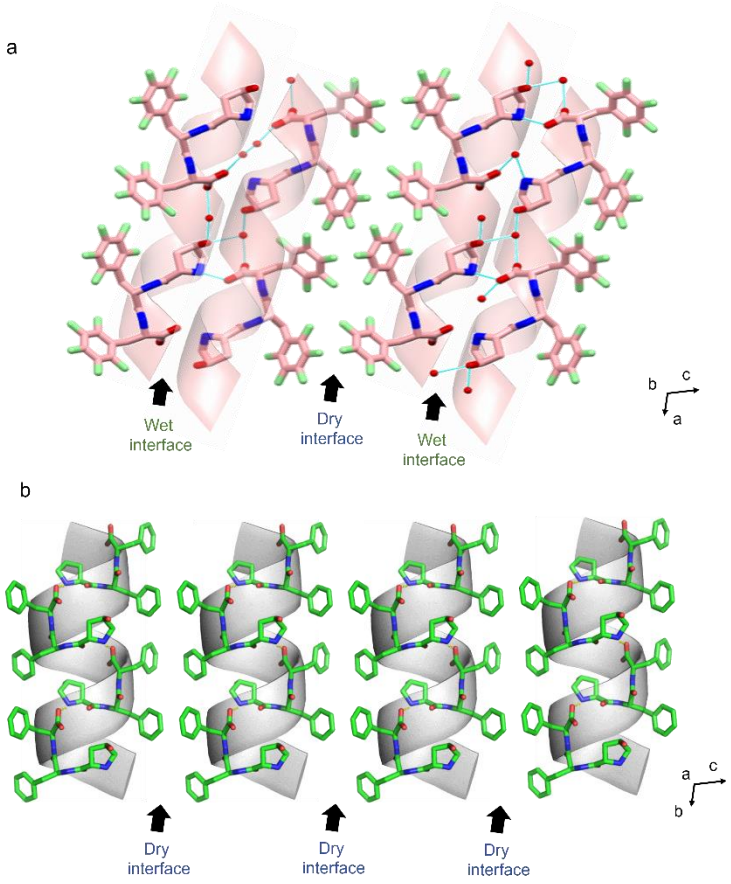

Figure S2. a,b) The crystal packing of Hyp-F_5Phe-F_5Phe (a) vs Hyp-Phe-Phe (b). The crystal packing is shown down the fibril axis, here four rows of sheets are presented. For Hyp-F_5Phe-F_5Phe, the packing depicts the alternating hydrophobic and hydrophilic interfaces between rows of sheets. The middle rows of pair of sheets featuring the hydrophobic dry interface lacking water molecules, represents the basic unit of fibrils. This rows of pairs of sheets are fully separated by wet interfaces lined with water molecules. For Hyp-Phe-Phe, all the four rows of sheets interact through hydrophobic interactions as

both the faces of a sheet extend aromatic side chains. Thus, there is continuous stacking of sheets and increased diameter of the resulting fibrils.

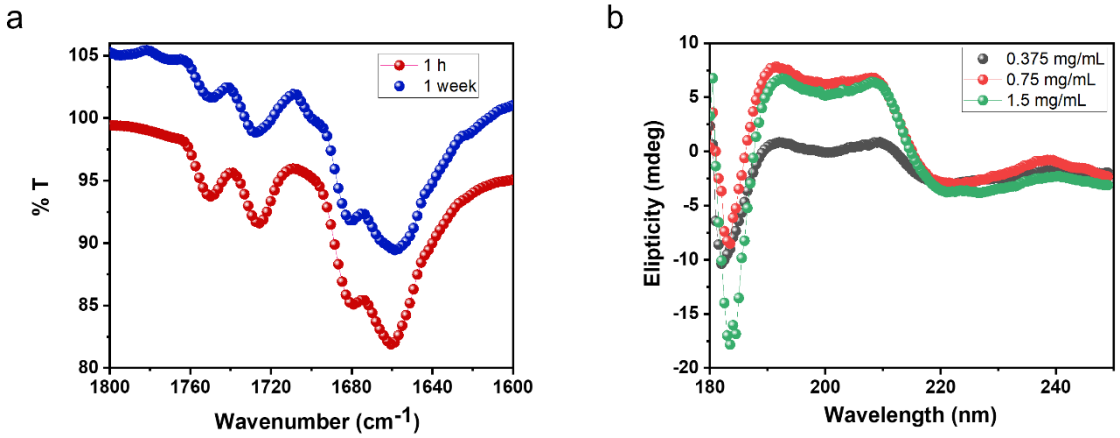

Figure S3. a) Time-dependent FTIR spectra of Hyp-F_5Phe-F_5Phe. The data of 1 h recorded from sample prepared after dissolving peptide in organic solvent (DCM) and quickly dried under heating (at 60º C). b) Concentration dependent CD spectra of Hyp-F_5Phe-F_5Phe.

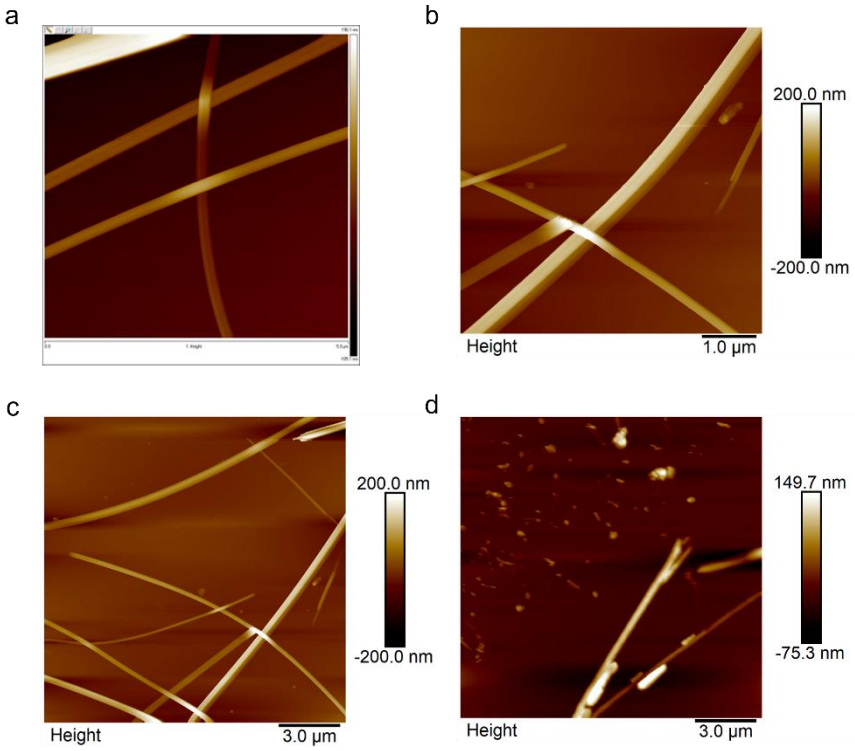

Figure S4. AFM images of the Hyp-F_5Phe-F_5Phe demonstrating amyloid-like fibrillar morphology. a) The raw, unprocessed AFM images of Figure 2d. b-d) Images captured in dry (b,c) and hydrated (d) state.

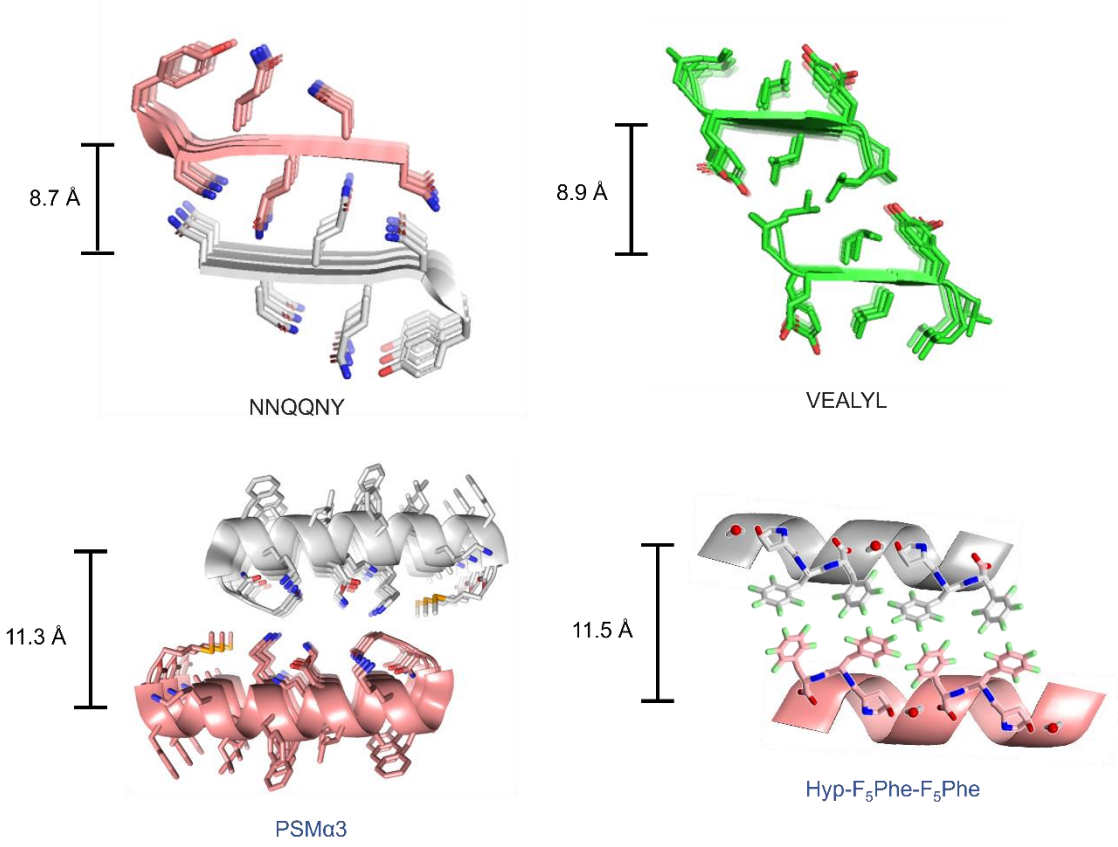

Figure S5. Distances between mating sheets in cross-β structure forming NNQQNY (PDB code 1YJO) and VEALYL (PDB code 2OMQ), and cross-α structure forming PSMα3 (PDB code 5i55) and Hyp-F_5Phe-F_5Phe.

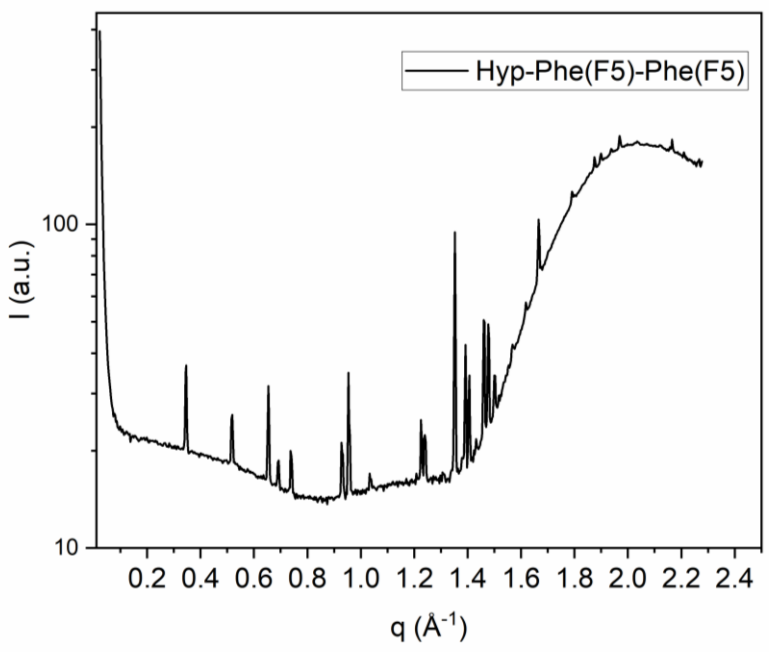

Figure S6. WAXS spectra of Hyp-F_5Phe-F_5Phe assemblies in aqueous suspension.

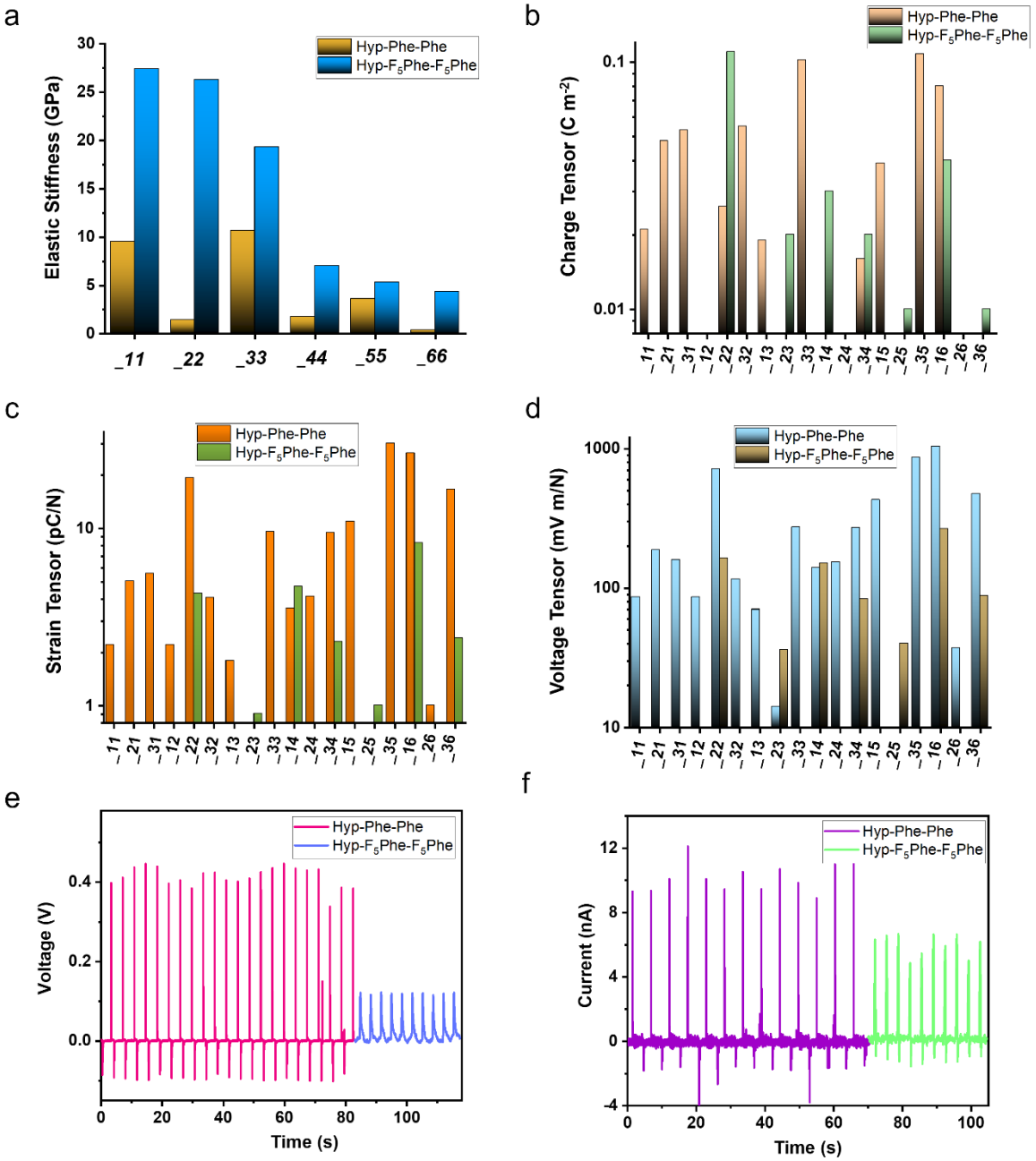

Figure S7. Comparison of piezoelectric output of Hyp-Phe-Phe and Hyp-F_5Phe-F_5Phe assemblies. a-d) DFT-predicted mechanical (a) and electromechanical (b-d) properties of peptide single crystals. e,f) Upon applying 23 N force, generated voltage (e) and current (f) output in the forward connection from the devices fabricated with Hyp-Phe-Phe and Hyp-F_5Phe-F_5Phe assemblies.

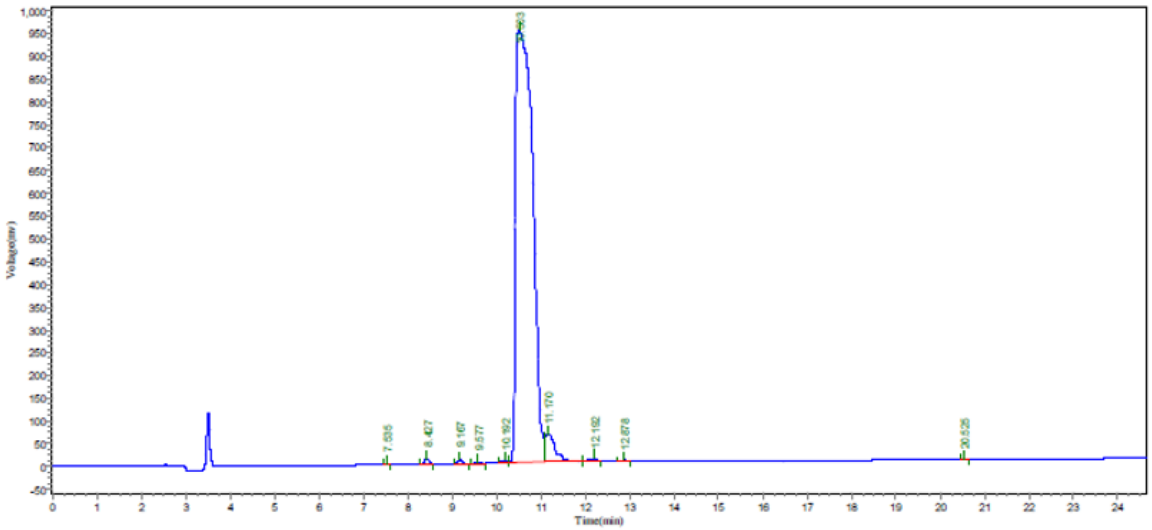

Figure S8. HPLC trace of Hyp-F_5Phe-F_5Phe.

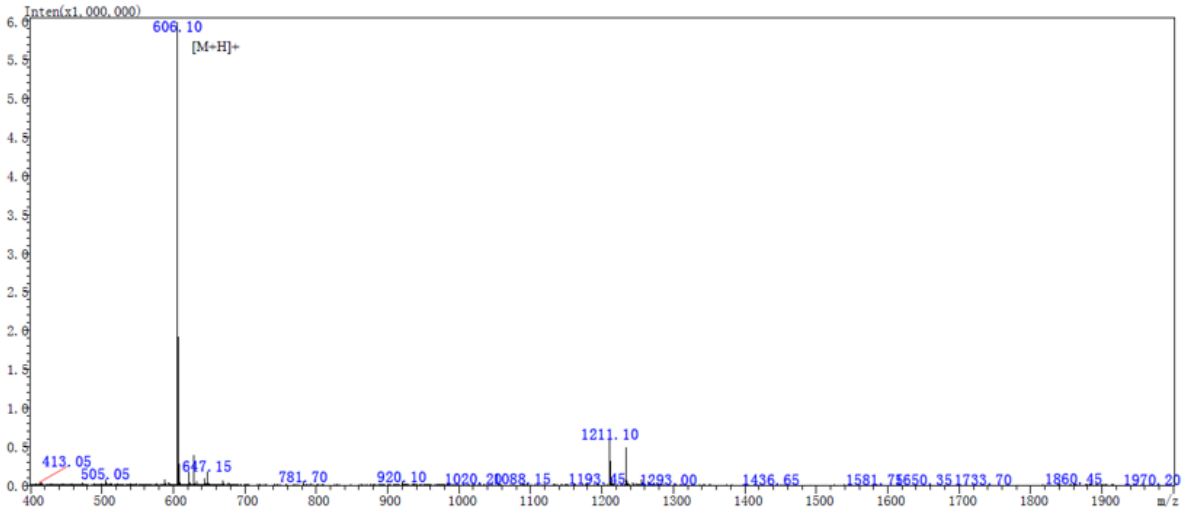

Figure S9. Mass spectra of Hyp-F_5Phe-F_5Phe.

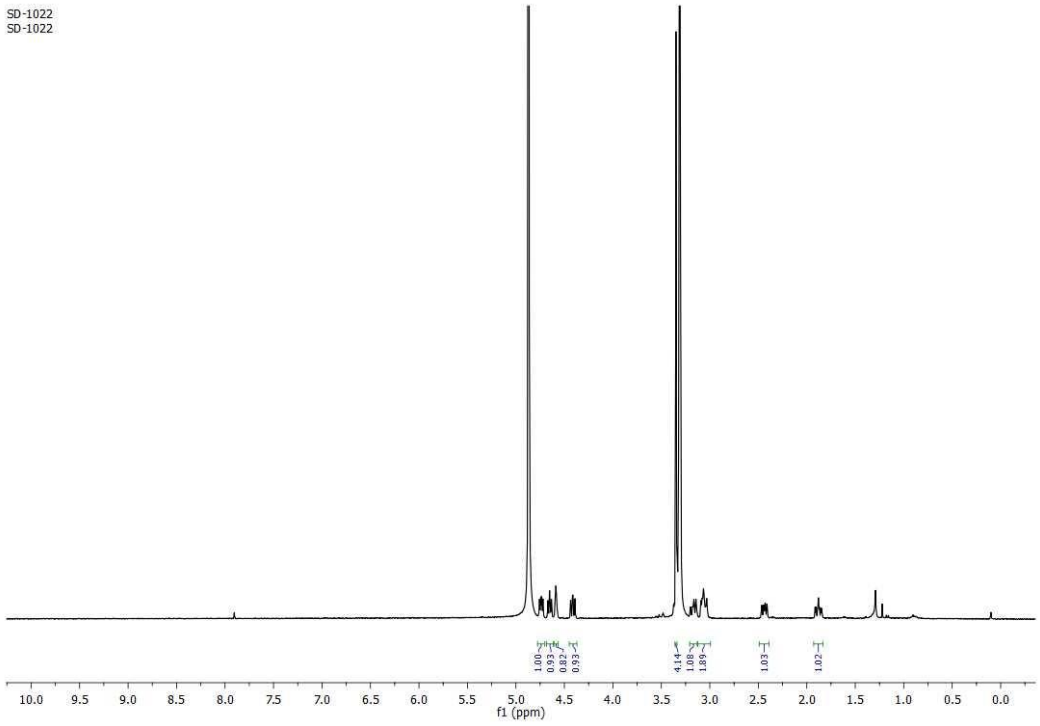

Figure S10. ^{1}H NMR (400 MHz, CD_3OD, δ_{ppm}) spectra of Hyp-F_5Phe-F_5Phe.

Supplementary Table S1: Torsion angles of F_5Phe2/Phe2 residue

Peptide	φ2	ψ2
Hyp-F_5Phe-F_5Phe	61.53°	79.23°
Hyp-Phe-Phe		
Molecule A	-71.1°	-43.2°
Molecule B	-70.5°	-41.9°

Supplementary Table S2: Data collection and refinement statistics

Experimental details:

Crystal data	Hyp-F_5Phe-F_5Phe
Chemical formula	C23 H21 F10 N3 O7
Mr	641.43
Crystal system	Monoclinic
Space group	$P2_1$
a (Å)	13.8220(5)
b (Å)	4.9037(2)
c (Å)	19.1807(7)
α (°)	90
β (°)	104.047(4)
γ (°)	90
V ($Å_3$)	1261.17(9)
Z , *Z*'	2
μ (mm^{-1})	1.611
Temperature (K)	100 (2)
Data collection	
Diffractometer	Rigaku XtaLAB AFC12 (RINC): Kappa dual home/near
Crystal size (mm)	0.081/0.013/0.011
Absorption correction	gaussian
*T*min , *T*max	0.891, 1.000
$N_{measured}$	18039
$N_{observed}$ [$I > 2\sigma(I)$]	4435
R_{int}	0.0392
θ_{max} (°)	70.075
Refinement	
$R[F2 > 2\sigma(F2)]$	0.0392
wR(*F*2)	0.1073
Goodness-of-fit	1.111
No. of reflections	4435
No. of parameters	395
No. of restraints	1
H-atom treatment	H-atom parameters constrained

Supplementary Table S3: Comparison of power outputs of PENGs based on different materials.

Type	Engineering methods	Current output (*I*)	Reference
MoS_2	Single-atomic-layer MoS_2	0.03 nA	1-6
	Point-defect-passivated MoS_2 nanosheet	0.1 nA	
	MoS_2 monolayer	47.5 nA	
	Cellulose/MoS_2 nanosheet	150 nA	
	Cellulose nanofibril/MoS_2 nanoshee	210 nA	
	TiO_2/MoS_2/PVDF	540 nA	
M13 bacteriophage	Bacteriophage	6 nA	7-10
	Vertically aligned bacteriophage	13 nA	
	Transient self-templating bacteriophage	93 nA	
	Vertically aligned and polarized bacteriophage	120 nA	
Fish skin collagen	Fish scale	1.5 μA	11-14
	Pollack skin	1.12 μA	
	Fish swim bladder	51 nA	
	Fish-skin	20 nA	

Refernces:

1. W. Wu, L. Wang, Y. Li, F. Zhang, L. Lin, S. Niu, D. Chenet, X. Zhang, Y. Hao, T. F. Heinz, J. Hone, Z. L. Wang, *Nature* **2014**, *514*, 470.
2. S. A. Han, T.-H. Kim, S. K. Kim, K. H. Lee, H.-J. Park, J.-H. Lee, S.-W. Kim, *Adv. Mater*. **2018**, *30*, 1800342.

3. A. Sohn, H. J. Hwang, P. Zhao, W. Kim, J.-H. Jung, L. Kang, D. Choi, S.-W. Kim, A*CS Appl. Mater. Interfaces* **2024**, *16*, 1317.
4. S. Chen, J. Li, Y. Song, Q. Yang, Z. Shi, C. Xiong, *Cellulose* **2021**, *28*, 6513–6522.
5. T. Wu, Y. Song, Z Shia, D. Liu, S. Chen, C. Xiong, Q. Yang, *Nano Energy*, **2021**, *80*, 105541.
6. A. Bhatt, V. Singh, P. Bamola, D. Aswal, S. Rawat, S. Rana, C. Dwivedi, B. Singh, H. Sharma, *J. Alloys Compd.* **2023**, *960*, 170664.
7. B. Y. Lee, J. Zhang, C. Zueger, W.-J. Chung, S. Y. Yoo, E. Wang, J. Meyer, R. Ramesh, S.-W. Lee, *Nat. Nanotechnol.* **2012**, *7*, 351.
8. D. M. Shin, H. J. Han, W. G. Kim, E. Kim, C. Kim, S. W. Hong, H. K. Kim, J. W. Oh, Y. H. Hwang, *Energy Environ. Sci.* **2015**, *8*, 3198.
9. K. Heo, H.-E. Jin, H. Kim, J. H. Lee, E. Wang, S.-W. Lee, *Nano Energy* **2019**, *56*, 716-723.
10. J.-H. Lee, J. H. Lee, J. Xiao, M. S. Desai, X. Zhang, S.-W. Lee, *Nano Lett.* **2019**, *19*, 4, 2661–2667.
11. S. K. Ghosh, D. Mandal, *Appl. Phys. Lett.* **2016**, *109*, 103701.
12. H.-Y. Son, S.-S. Park, Mater. Today Sustain. **2024**, *25*, 100689.
13. S. K. Ghosh, D. Mandal, *Nano Energy* 2016, 28, 356.
14. S. K. Ghosh, D. Mandal, *ACS Sustainable Chem. Eng.* **2017**, *5*, 8836.